PAPER 81 - EFFECTS OF AERO-ENGINE DEGRADATION ON SPECIFIC FUEL CONSUMPTION AT VARYING AMBIENT AND TURBINE INLET TEMPERATURES

I.O. OTAIKU[1], I. K. ADEGUN[2]

International Aviation College, Ilorin, Kwara State and Kwara State University
Department of Mechanical Engineering, University of Ilorin, Ilorin, Nigeria
Corresponding Author: olaoluwa.otaiku@gmail.com. +23460520474.

ABSTRACT

The paper presents the effects of aero-engine degradation on specific fuel consumption at varying ambient temperature and turbine inlet temperature. The ambient and turbine inlet temperatures were varied using analytically developed equations. These parameters with the specific fuel consumption, were modelled to determine the performance of the engine at each instance. A 4- stage compressor and a single stage turbine were investigated for 0 to 10% area reduction of the blades. Increase in degradation and margin to permanent failure were examined. The ranges of ambient and turbine inlet temperatures and TIT considered were 295 to 325 K and 1083-1245 K respectively. specific fuel consumption against ambient and turbine inlet temperatures, mass flow rate and net power produced at each level of blade degradation were plotted. Results showed that for undegraded compressor blades, the changes in the ambient did not have significant effect on the compressor's exit temperature. However, at 8% blade degradation, the effect was noticeable and became risky at 10%, where the exit temperature seemed to be increasing beyond tolerable temperature of the material. It was also observed that SFC increased with increasing TIT. The results predict that margin to permanent failure of the engine would occur at 10% compressor's blade degradation when the SFC would have risen to 0.5 kg/kWh, ABT (315 K), TIT (1100 K) and fuel flow rate at 0.4 kg/s. In conclusion, to prevent complete engine-out, the revolution per minute of the engine at these conditions should be reduced to 80% and landing procedures initiated.

KEYWORDS: Specific fuel consumption (SFC), ambient temperature (ABT), turbine inlet temperature (TIT) and surface area degradation.

1. INTRODUCTION

The interpretation of the degraded engine performance has been reported by De Castro-Cros et al. (2023) that SFC is one of the parameters to depict an engine nearing an end to active service life cycle. Therefore over-fuelling during different phases of flight especially climb for a degraded engine could cause high temperature and thermal shock which is undesirable at such phase because it increases the fatigue due to centrifugal stress on the engine and can accelerate the deteriorating operation of the compressor close to the choking condition or surge (Kolias et al., 2021). If no remedy is quickly applied at the instance of transient or dynamic condition, compressor operating condition will move the engine from large to very small margin to surge that can result to complete flame out and badly damaged engine (ATSB, 2014). The aim of this study is therefore to carry out an analytical modelling by developing equations for the rate of change of SFC during the engine degradation relative to varying ambient and turbine inlet conditions.

1.1.Turbomachinery of the Compressor and the Turbine

Deterioration of aero-engine gas turbine blades affects their exit angles, length and other parameters of the blade profile which will definitely result to increase in unexpected losses. It has been reported by Otaiku and Adegun (2021); Kurzke, J.; Halliwell (2018); Alexiou (2020); Aungier (2003) and Zhang et al. (2020) that the main influence of degradation appears around the optimum incidence angles. If the leading edge of the blades experience above 10.04 mm crack or fracture according to AMM (P & W 2014), there will be increase in flow of air/gas thereby over building up the pressure within the control volume above the specified range (choked condition) and causing a progressive turbulent flow and negatively affecting the work output and efficiency of the engine. As long as this new condition persists, the rotational speed of the driving shaft will definitely reduce performance until the process eventually move from turbulent flow to separation of flow around the degraded blades (Hendricks 2016) with significant loss in aerodynamic property of the airfoil blade. It should be noted at this point that in the compressor section, ambient air temperature plays a vital role in the exit temperature of the compressor. So, at higher ambient temperature for a degraded blades in the compressor, the greater the compression ratio and the more the fuel being consumed at the combustion section due to reduction in the effective (pressure) surface area of the blades and blockages according to

Otaiku and Adegun (2023). For an ideal engine, by assuming a constant temperature rise across all the stages in the compressor, the ambient temperature ranges do not significantly affect the compressor exit temperature when the aforementioned condition apply. But in cases of engine degradation, where the temperature per stage depends on the condition of the blades per stage, then one can expect a paradigm shift of the general assumption and determination of effect of ambient temperature on degraded blades per stage in the compressor and turbine is imperative. reason why this study is carried out.

1.2 Literature Review

Singh et al. (1999) presented a model and sample calculations for the deterioration of three different single stage compressors. The presented model included the effects of increased roughness and tip clearance due to erosion, resulting to losses and poor performance of the engine. However, they omitted the amount or percentages of surface area reduction due to reducing length of the blades that cause the losses. This gap has been adequately covered in this study.

De Castro et al. (2023) carried out experimental study of the performance of the compressor at the degraded condition, their results showed how there is need to install autoencoder on the engine to help to define an indicator of the compressor behaviour in long-term performance. They analysed the condition and performance of a gas turbine after a maintenance operation using two different autoencoder architectures. Their results showed that there is need to install a fuel flow control system to maintain the fuel flow schedule such that the engine will not run into risky operating conditions due to change in fuel flow and increase in SFC for a degraded engine (e.g. where the compressor working line would cross the surge margin). Goeing et al. (2020); Srinival et al. (2018) and Xin et al. (2019) explained that the effect of compression ratio on compressor work is similar to turbine work. As the work increased with increase in the compression ratio, it was expected that the ambient temperature also increased. A low ambient temperature produced high air density and a high gas turbine compressor work and output power and also a higher SFC.

Bayona-Roa et al. (2019); Liu et al. (2021) and Egorov et al. (2018) carried out experimental and numerical work on degraded blades' performance of the aero-engine with variation in ambient temperature as a function of compressor work output thereby significantly affecting the thermal efficiency of the engine. As the ambient temperature increased, the thermal efficiency decreased. This was because, the air mass flow rate inlet to compressor increased with decrease of the ambient temperature. Their result showed that at 90% design speed, the losses in efficiency and pressure ratio were high due to fractured area or the blade surface. It was also noticed that there was a reduction in efficiency of 22% as compared to that of on design configuration. Also, findings showed the total pressure, efficiency and the mass flow rate at the near stall condition at 80% design speed, as compared to the design point parameters. This study has clearly brought out that the margin to surge in the compressor stage was any speed less than 85% of the design speed.

Foorozan et al. (2015) explained that the compressor and turbine mass flow rates varied similarly to the fuel consumption rate. That is, the transient response that existed in the compressor as the blade deteriorated, caused the mass flow to reduce and fuel flow becoming higher thereby consuming more than necessary.

2. THEORETICAL ANALYSIS

For a given speed of a degraded compressor and turbine, higher temperature and an increased axial velocity component will emerge because of reduced pressure. The equation for such pressure is as shown in Equation 1:

$$p=\rho RT \quad (1)$$

Inlet conditions, such as total inlet pressure, total inlet temperature (ambient temperature), inlet Mach number, and the inlet flow angle are calculated as given in Equations 2 and 3. The Inlet static pressure, inlet static temperature and inlet speed of sound can be found using isentropic relationships as shown in Equations 4-7 (Cohen et al., 1996; Farokhi, 2013 and Saravanamuttoo et al., 2009)).

$$P_t = P_1\left(1+\frac{\gamma-1}{2}M^2\right)^{\frac{\gamma}{\gamma-1}} \quad (2)$$

$$T_t = T_1\left(1+\frac{\gamma-1}{2}M^2\right)^{\frac{\gamma}{\gamma-1}} \quad (3)$$

Where Pt is the inlet total pressure, Tt is the inlet total temperature, P1 is inlet static pressure, T1 is inlet static temperature, γ is the specific heat ratio, and M is the inlet Mach number which is usually < 1.

The relative velocity VR of the flow over the blade, inlet speed of sound and the Mach number relationship are as given in Equations 4-6.

$$V_R = Ma \quad (4)$$

$$a = \sqrt{\gamma RT} \quad (5)$$

$$V_R = M\sqrt{\gamma RT} \quad (6)$$

The mass flow of air/gas in the compressor and turbine is as given in Equation 7.

$$\dot{m}_a = \rho AV \quad (7)$$

From the first law of thermodynamics and the Euler turbine equations, the work done W, enthalpy h, absolute velocity V and the relative total temperature ratio are as shown in Equations 8 -9. Also, from the Euler turbine equation, work in terms of wheel speed, relative velocity, and absolute velocity is as given in Equation 9.

$$W = \left(h_2 + \frac{V_2^2}{2}\right) - \left(h_1 + \frac{V_1^2}{2}\right) \quad (8)$$

$$W = \frac{1}{2}[(U_2^2 - U_1^2) - (V_{R2}^2 - V_{R1}^2) - (V_2^2 - V_1^2)] \quad (9)$$

where h_1 and h_2 are enthalpy at the inlet and exit respectively, V_1 and V_2 are absolute velocity at the inlet and exit, respectively. Where U_1 and U_2 are wheel speed at the inlet and exit, respectively. If we set equations 8 and 9 as equal to each other, the absolute velocities cancel out. From the velocity triangles as presented by Farokhi, (2013) and Saravanamuttoo et al., (2009) the stagnation temperature at the compressor or turbine can also be obtained from Equation 10.

$$T_t = T_1 - \frac{U^2}{2c_p}\left\{\frac{\Delta h}{U^2} + 1 - 2R_n\right\} \quad (10)$$

3. METHODOLOGY

The thermodynamic and Euler equations as shown in the previous section were further remodified to suit the assumptions made in this study. The new equations developed is derived from the fundamental equations and key parameters such as SFC, mass and fuel flow rates, engine efficiency and power at different shaft speed were obtained as analytical data and further plotted for explicit presentation. This is also shown in the Appendix A.

3.1. Preliminary Assumptions

a. Ideal gas properties and Sea level static (SLS) conditions for compressible fluid were considered and the compression and the expansion are adiabatic and isentropic.

b. Rate of change of density equals zero.

c. Axial directional flow was considered (x-direction).

d. NACA 65-(18)10 model was adopted for developed blade models.

e. 0 to 10% reduction in original blade area was assumed to be radial for rotating condition and elongation or blade fracture was vertically from the tip to the hub.

f. The heating value of the fuel is 43MJ/kg.

The degraded blade region is as shown in Figure 1 b and c.

3.1.1. Governing Equations

The unsteady 3-D flow of compressible fluid in compressor and turbine sections can be converted to 1-D to form the conservation of mass and energy as shown in Equations 11 a, b and 12.

3.1.2. Conservation of Mass

$$\frac{\partial \rho}{\partial t} + \frac{\partial}{\partial t}\rho u + \frac{\partial \rho}{\partial t}\rho v + \frac{\partial \rho}{\partial t}\rho w = 0 \quad 11a$$

$$\frac{\partial \rho}{\partial t} + \nabla.(\rho V) = 0 \quad 11b$$

Where velocity field vector in v and w = 0

Conservation of Energy

$$\frac{\partial \rho e}{\partial t} + \nabla.(\rho e V) \quad 12$$

3.1.3. Determination of Damaged Blade Surface Area

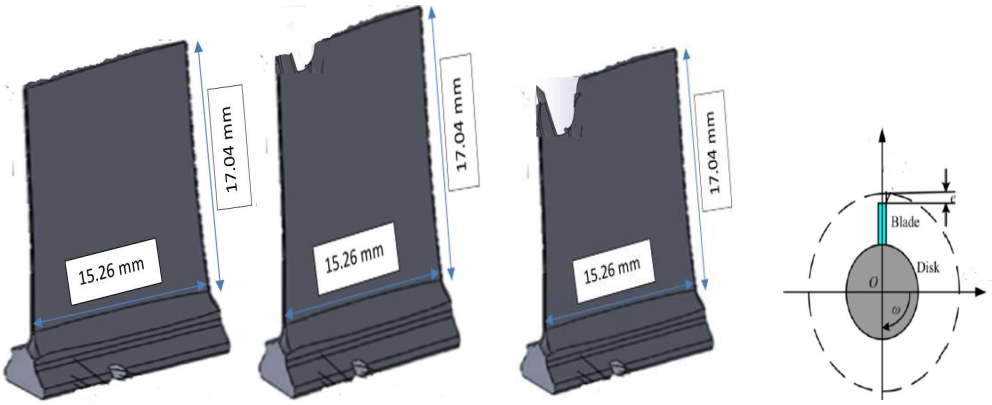

a. 0% undegraded blade b. 8% degraded blade and c. 10% degraded blade. d. Blade on the turbine disk.

Figure 1: Blade Specimen

3.2 Rotating Blade (without degradation or 0%).

The Figure 1 d shows the mounted blade on the disk and as given in the assumption, the radius of the blade with changing length is as shown in Equations 13 and 14.

radius at the tip $r_0^i = \frac{1}{2} l_0(t) + r_0(t)$ 13

- radius at the root $r_h = r_0(t)$ 14

3.2.1. Rotating Blade (8 to 10% degradation in surface area)

The new radius at the tip of the leading edge after fracture or break away is obtained from Equation 15.

$$r_{new}^i = \pi \left(\frac{1}{2}\bar{l}_{new} + r_0\right)^2 \quad 15$$

Based on the assumptions earlier stated and equations 11 a, b and 12, other fluid characteristics flowing around the rotating blades (0-10%) were derived as shown in Equations 16-17.

Note: The blade parameters were obtained by the empirical calculations and used for its development using SOLIDWORKS 20.

3.3. Derived analytical equation for the fluid

The law of conservation of mass from Equation 11 yields the mass flow rate, so for rotational transient conditions in x- direction (AL-Luhaibi and Tariq (2014)),

$$\dot{m}_{in} = \dot{m}_{out} = \rho\, V_{a1}\, \pi \left(\frac{1}{2}\bar{l}_{new} + r_0\right)^2 = \rho V_{a2}\, \pi \left(\frac{1}{2} l_0(t) + r_0(t)\right)^2 \quad 16$$

Multiplying linear velocity u with Equations 11 and 12 yields conservation of momentum is equal to conservation of energy rate

$$(\dot{\rho}ue + \rho\dot{u}e)V = (\dot{\rho}u + \rho\dot{u})V \quad 17$$

Also, derived equations for net power $\dot{W}$ and Torque τ are derived from Equation 17 to yield Equation 18

$$\dot{W} = P_t - P_c = \tau\omega = \dot{m}(U_1\Delta V_{\alpha 2} - U_2\Delta V_{\alpha 1}) \quad 18$$

3.4 Effect of density change on pressure change

General equations shown in Equations 1-7 for mass, density, pressure, temperature and Mach number are further modified to form Equations 19 -20 as required for this study.

- $$\rho = \frac{P_1\left(1+\frac{\gamma-1}{2}M^2\right)^{\frac{\gamma}{\gamma-1}}}{R\left(T_1\left(1+\frac{\gamma-1}{2}M^2\right)^{\frac{\gamma}{\gamma-1}}\right)} \quad 19$$

Mass flow rate for changing density and pressure with degraded blades

$$\dot{m_a} = \frac{P_1\left(1+\frac{\gamma-1}{2}M^2\right)^{\frac{\gamma}{\gamma-1}}}{R\left(T_1\left(1+\frac{\gamma-1}{2}M^2\right)^{\frac{\gamma}{\gamma-1}}\right)}\pi\left(\frac{1}{2}\bar{l}_{new} + r_0\right)^2 M\sqrt{\gamma RT_1\left(1+\frac{\gamma-1}{2}M^2\right)^{\frac{\gamma}{\gamma-1}}} \quad 20$$

3.5 Specific Fuel Consumption for degraded compressor and turbine blades

From Kolias et al. (2021); Henrique et al. (2020); Foroozan et al. (2013) Kurzke (2011); Saravarramutto (2014) and Farokhi (2013), SFC for the degraded sections is as given in Equation 21.

$$SFC = \frac{3600\,x\,m_f}{\dot{W}_{net}} \quad 21$$

$$\eta_{th} = \frac{\dot{W}_{net}}{LCV.m_f} \quad 22$$

From Equations 16 and 21 and based on the assumptions considered, Equation 23 was derived for change in Specific Fuel Consumption of the degraded engine as ambient and turbine inlet also change as $SFC =$

$$\left\{300 * \frac{mf}{c_p * \pi\rho_i V_{zi}\left[1+\frac{1}{\left(1+\frac{r_t}{r_h}\right)}\right]}\right\}/(T_1 + T_3 - (T_2 + T_4)) \quad 23$$

3.6. Thermal Efficiency

One other key parameter that should not be ignored is the thermal efficiency for the degraded engine. So combining Equations 16, 18 and 20, Equation 24 is obtained for thermal efficiency.

$$\eta_{th} = \frac{c_p * \pi\rho_i V_{zi}\left[1+\frac{1}{\left(1+\frac{r_t}{r_h}\right)}\right]}{LCV.m_f} \quad 24$$

Compressor: Ambient temperatures T_1 (288 to 343K), exit temperatures T_2 = 535 to 560 K. Turbine: Turbine Inlet Temperature was set between T_3 (1093 to 1245 K), exit temperatures T_4 = 870 to 1100 K.

4.0. RESULTS AND DISCUSSION

4.1.1. Compressor Section

The compressor section comprised a 3-stage axial, single stage centrifugal with rotor speed of 38,100 RPM and air pressure ratio of 7.7. The total inlet and outlet pressure, inlet and exit temperatures were 101325 Pa and 759937.5 Pa (shown in Figure 2), 298 to 325 K and 560-563 K from the entire compressor which will be presented graphically in

the next session. A typical value for the exit temperature of compressors is 560K as validated from Bela (2018) for a steady state compressor operation as represented in this study with 0% degradation. **T**emperature rise per stage was obtained to be 1.77 K and assumed to be constant across each stage. Taking the inlet total pressure as 101325 Pa for the damaged and undamaged blades, the compressor exit pressure for 8% and 10% reductions in surface areas were 8 MPa and 10 MPa with overall compressor ratio dropping from 7.7 to approximately 3.16 as shown in Figures 2, 3 and 4.

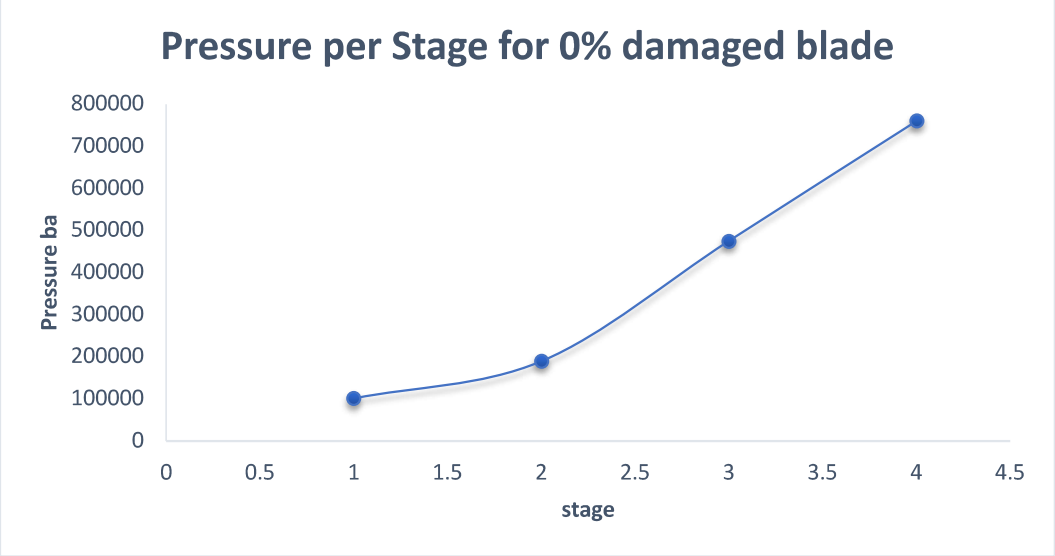

Figure 2: Pressure increase per stage for 0% degradation.

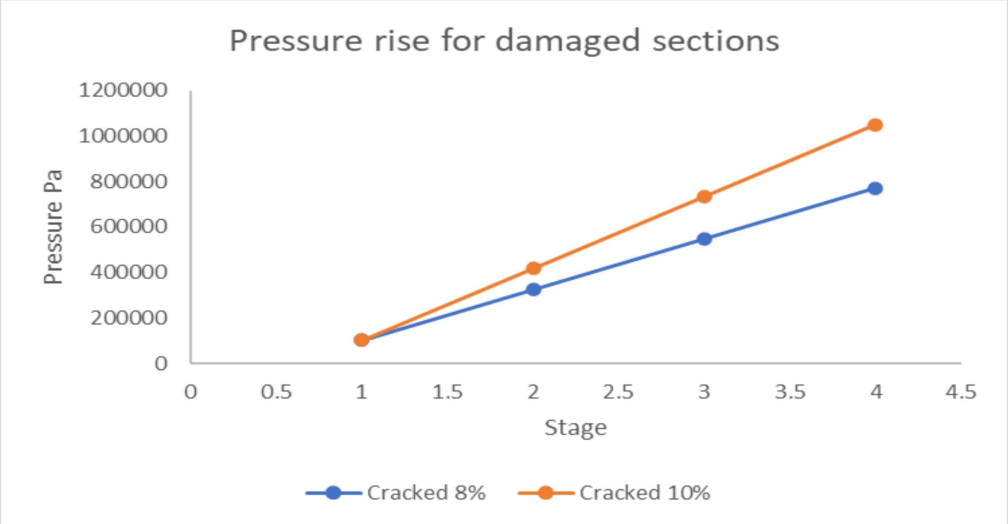

Figure 3: Pressure increase per stage for 8 and 10% degradation.

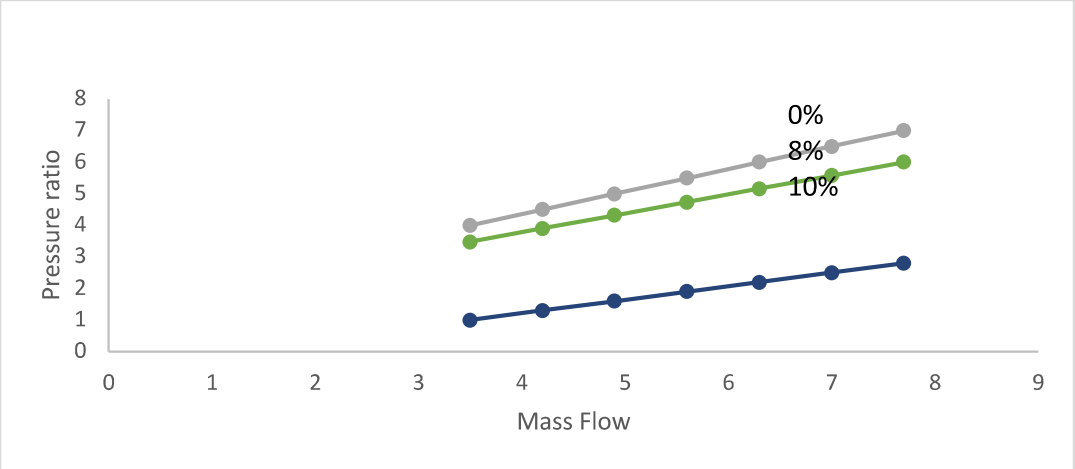

Figure 4: Pressure ratio vs mass flow rate

4.2. Effect of Change in Ambient Temperatures

Effect of ambient temperature on undegraded and degraded 4- stage compressor is as shown in Figures 5-6. For 0% degradation, the compressor exit temperature was obtained as approximately 563 K according to Figure 5 as validated from Bela (2018) which has earlier been mentioned. Particular attention is paid to the performance of the compressor as regards to actual temperature that was expected from the undegraded and degraded as shown in Figures 6 a and b respectively. The expected performance is that all the stages of the compressor and the turbine were working at their optimum efficiency point at design surge margins. But in the event of noticeable degradation, all the stages will start to work at off optimum surge margins and lower than design efficiency (Otaiku and Adegun, 2023 and De-Castro et al., 2023). Also, the losses will increase as the flow increases. However, if the degradation of the turbine section leads to material removal as been studied here and presented experimentally by Otaiku and Adegun, (2023), especially in the rotor area, the flow capacity increases for any given pressure ratio. Leading edge degradation in the turbine especially causes a shift in the distribution of pressure ratios i.e., a larger portion of the overall pressure ratio is consumed by the gas generator turbine (Bayona-Roa et al. (2019);Xin et al. (2019); Rahman and Whidborne (2008); Bonet and Pilidis(2013); Saravanamuttoo et al. (2009); Kurz et al. (2019); Cruz-Manzo et al. (2020); Kauth et al. (2019) and Goeing et al. (2020); Saravanamuttoo et al. 2009; Kurz et al. 2019). This causes a shift in the corresponding turbine inlet temperature to higher ambient temperatures as shown in Figures 6 a and b for 8 and 10% degradation.

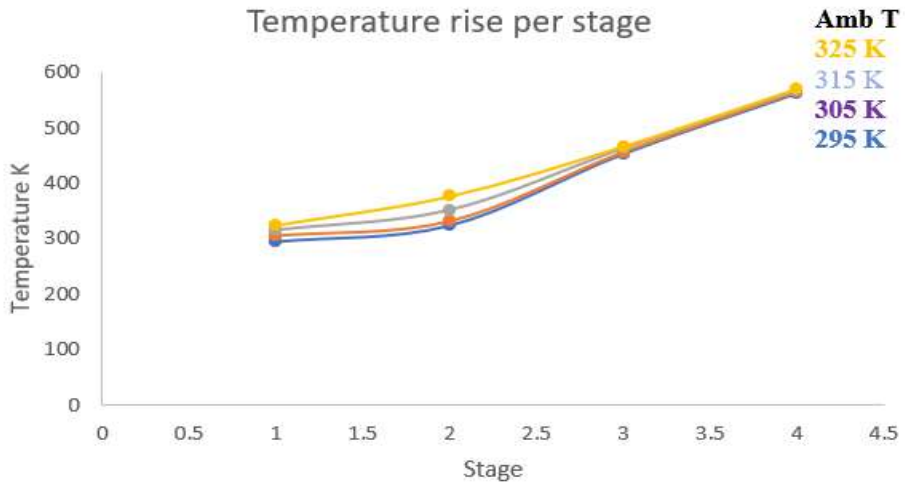

Figure 5: Ambient temperature change vs compressor exit temperature

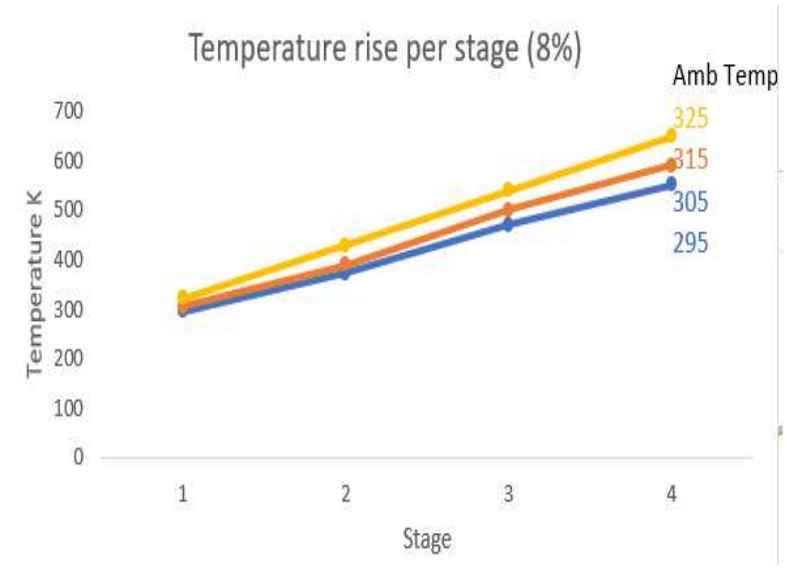

a. 8% degradation

b. 10% degradation

Figure 6 a and b: Ambient temperature change with significant effect on compressor exit temperature.

4.3. Effect of Ambient Temperature on Specific Fuel Consumption and Turbine Inlet Temperature for degraded compressor and turbine.

Figure 6 shows the condition of the engine in terms of rate of specific fuel consumption with increasing ambient temperatures for 0, 8 and 10% reductions in blade length and surface area at both the compressor and the turbine. SFC obtained for 0% degraded blades was approximately 0.365 kg/kWh for ambient temperatures (295 to 315 K) and TIT 1083 K as shown in Figure 7. However, due to the degradations, the SFC will rise to 0.4 and 0.5 kg/kWh respectively as TIT increases as shown in Figures 7 and 8. Also, this will prompt the reduction in engine power from 1183 kW and continuously decreasing below 1000 kW which is already at surge margin (Figure 8). Of course, at these new conditions of the blades during climb, excessive fatigue is imposed on the engine as more SFC will be needed to augment the net power loss thereby allowing undesigned increase in PR for an increase in TIT as shown in Figure 9. This is a stage that a complete engine out is reached and the entire engine is already lost. These dynamic events are as shown in Figures 7 - 9.

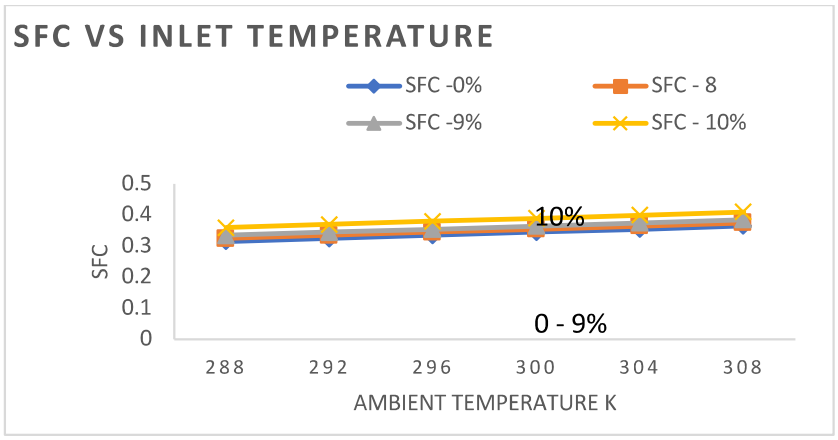

(a) SFC vs Ambient Temperatures

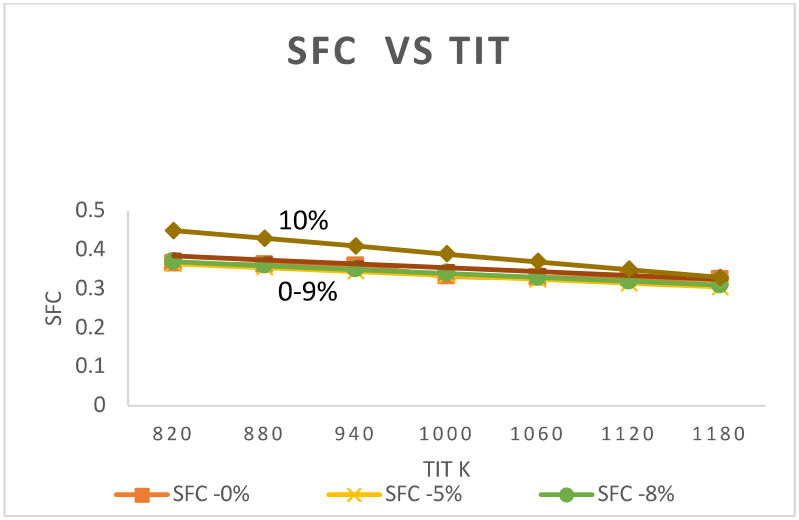

(b) SFC vs TIT

Figure 7 a and b: Change in ambient temperatures on SFC and TIT.

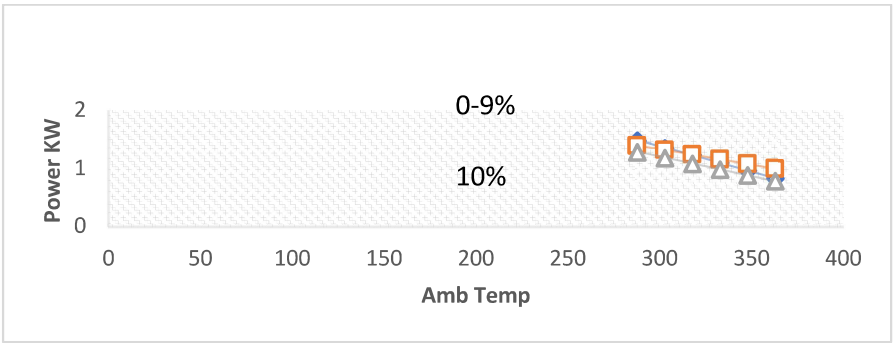

Figure 8: Change in power vs change ambient temperature

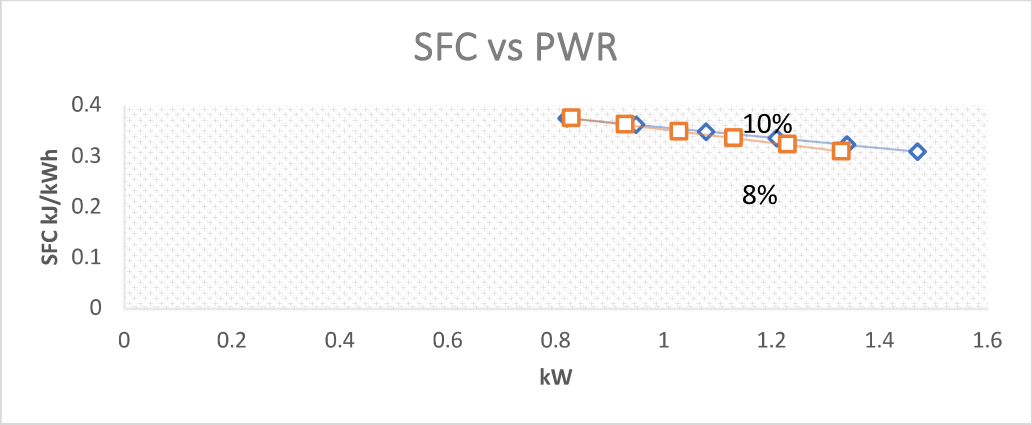

Figure 9: Increase in SFC vs decrease in power

4.4. **Effect of Pressure Ratio on Fuel Flow rate for change in Ambient Temperature**

As already being explained, the exit temperature of the compressor will definitely determine TIT that is the temperature leaving the combustion section (though not covered in this study). TIT according to the engine manufacturer must not exceed 1083 K for continued operation. However, going by this study, this condition will defiantly change due to change in the geometrical profile of the blade by reduction of it length and surface area which has been characterized as 8 and 10% degradation. Previously, the exit temperature increasing astronomically to maximum value of 600 and 750 K respectively at these new conditions. This transient response would increase as the deterioration continues. From Figures 10 and 11, the engine speed in RPM, pressure ratio, power, mass flow rate responses with the fuel flow rate and SFC which eventually result to surge at 10% reduction in surface areas of the blades in the compressor. The 10% area reduction and beyond showed that the turbine and compressor flow rates were non-uniform thereby aggravating the fuel flow in the combustion section.

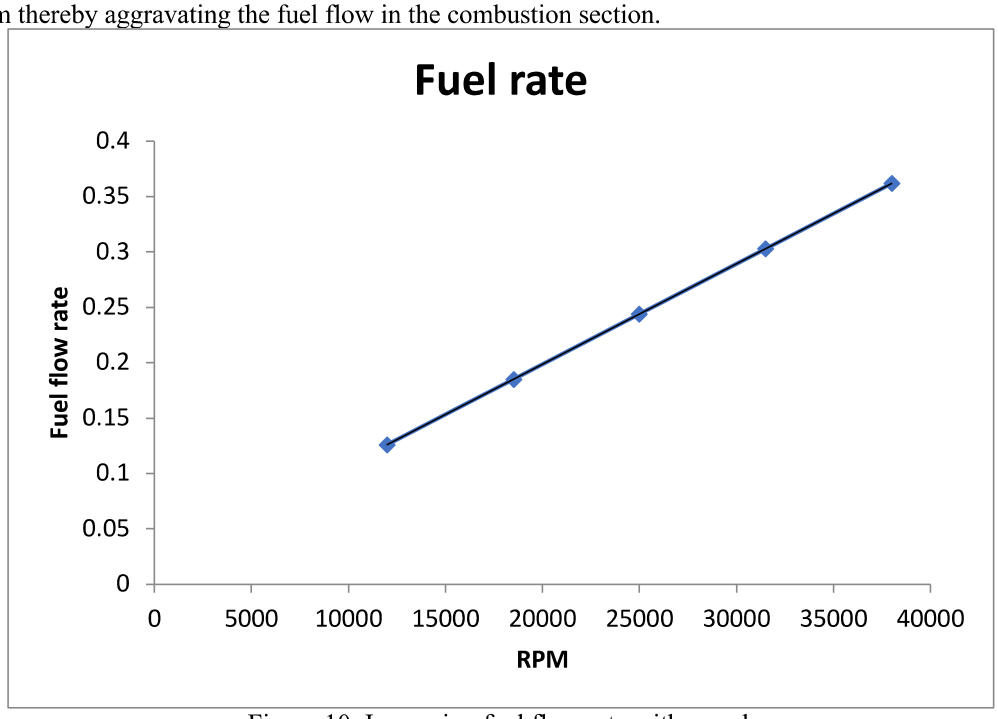

Figure 10: Increasing fuel flow rate with speed.

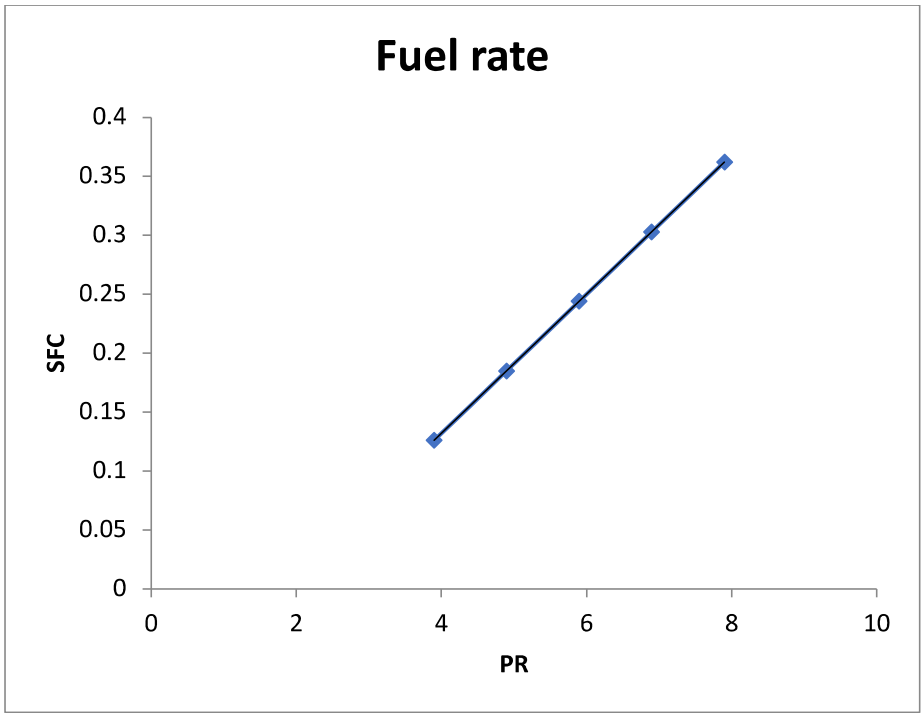

Figure 11: SFC increasing with PR

The resultant effect is that the specific fuel consumption SFC increases with the increase in ambient temperature. Under these abnormal conditions, losses in the burner section would be seriously noticed when the exit pressure and temperature at the compressor become higher for deteriorating engine thereby indicating a sudden increase in SFC an indication that the compressor section has been severely damaged (Moliere et al., 2020). This could have resulted from the blades crack or fracture as shown in the Figure 1 as earlier mentioned. The thermal efficiency also decreases with increase in air to fuel as corroborated by Rahman et al. (2011) and Moliere et al. (2020). This new development of the engine condition will cause choking at lower flow in both sections and a possibility of flow from the turbine back to the compressor a phenomenon called surge thereby shutting down the affected engine.

5. CONCLUSION

Effect of varying ambient and turbine inlet temperatures on specific fuel consumption for aero-engine with degraded blades have been studied and found to be significant. So effect of varying ambient temperatures for 8 – 10% blade surface area degradation of the compressor and turbine will affect the SFC, TIT, power output and the overall engine performance significantly especially at temperatures > 315 K. Compressor degradation usually cause higher power losses due to higher compressor exit temperatures as found to be between 600 and 700 K for 8 and 10% degradation respectively as against the validated value of 560 K which is categorized in this study as 0% degradation. Point of note is that SFC will increase with increasing turbine inlet temperature (TIT) particularly above 1100 K. The margin to permanent failure of the engine occurs at SFC of 0.4 kg/kWh, and TIT of 1100 K. Therefore operating the PT6T-turboshaft engine at these parameters could lead to permanent failure of the engine.

6. RECOMMENDATIONS

Therefore, from this study, the effect of degradation of blades up to 10% reduction in surface area has been studied and temperatures below 315 K ambient temperatures is somewhat recommended during flight to safely fly the aircraft to a final approach landing and should not exceed 315 K if the life of the engine is to be spared for the remaining stage of flight. In the event of stall before surge during flight operations, the maximum engine RPM should not exceed 80% and TIT not above 1092 K. However, if noticed on ground, whenever SFC is increased above the aforementioned values, the engine should be retired to the apron and internal failure of the blades should be ascertained and taking to the manufacturer for a complete replacement.

8. ACKNOWLEDGEMENT

The authors would like to thank University of Ilorin especially Profs, AGF Alabi, Aweda and Alao for their advisory role. Also worthy of note is Tgt. Rasheed from Kwara State for providing laboratory facilities for the simulation and experimental results respectively. Also, very special thanks to Petroleum Technological Development Fund (PTDF) for the financial support for my Ph.D work and Police Air Wing Abuja (ACP Ndubuisi and Engr. Cosmos Eze).

7. Conflict of Interest

The authors declare that no conflicting interest.

8. Data Availability

Operating data from the Aircraft Maintenance Manual from the manufacturer was used.

9. REFERENCES

De Castro-Cros, M.; Velasco, M.; Angulo, C. (2023). Analysis of Gas Turbine Compressor Performance after a Major Maintenance Operation Using an Autoencoder Architecture. Sensors 2023, 23, 1236. https://doi.org/10.3390/s23031236

Kurz, R.; Meher-Homji, C.; Brun, K.; Moore, J.J.; Gonzalez, F. (2013). Gas turbine performance and maintenance. In Proceedings of the 42nd Turbomachinery Symposium; Texas A&M University, Turbomachinery Laboratories: College Station, TX, USA, 2013.

Cheng, C.;Wang, J.; Chen, H.; Chen, Z.; Luo, H.; Xie, P. A (2021). Review of Intelligent Fault Diagnosis for High-Speed Trains: Qualitative Approaches. Entropy 2021, 23, 1.

Fu, S.; Zhong, S.; Lin, L.; Zhao, M. (2021). A re-optimized deep auto-encoder for gas turbine unsupervised anomaly detection. Eng. Appl. Artif. Intell. 2021, 101, 104199

Kurzke, J.; Halliwell, I. (2018). Propulsion and Power, An Exploration of Gas Turbine Performance Modeling, 1st ed.; Springer: Berlin/Heidelberg, Germany, 2018; ISBN 978-3-319-75977-7.

Alexiou, A. (2020). Introduction to Gas. Turbine Modelling with PROOSIS, 4th ed.; Empresarios Agrupados International (EAI) S.A.: Madrid, Spain, 2020.

Aungier, R.H. (2003). Axial-Flow Compressors, A Strategy for Aerodynamic Design and Analysis, 1st ed.; ASME: New York, NY, USA, 2003; ISBN 0-7918-0192-6.

Hendricks, E.S (2016). Meanline Analysis of Turbines with Choked Flow in the Object-Oriented Turbomachinery Analysis Code. In Proceedings of the 54th AIAA Aerospace Sciences Meeting, San Diego, CA, USA, 4–8 January 2016; AIAA-2016-0119.

Zhang, Y.; Zhang, S.; Xiao, Y. (2020). Aerodynamic Performance Prediction of Transonic Axial Multistage Compressors Based on One-Dimensional Meanline Method. In Proceedings of the ASME Turbo Expo 2020, Virtual, Online, 21–25 September 2020; GT2020-14571.

Srinivas G., Raghunandana K., and Shenoy B Satish (2018). Axial-flow compressor analysis under distorted phenomena at transonic flow conditions, Cogent Engineering, 5:1, 1526458, DOI: 10.1080/23311916.2018.1526458.

Kolias, I.; Alexiou, A.; Aretakis, N.; Mathioudakis, K. (2021). Axial Compressor Mean-Line Analysis: Choking Modelling and Fully-Coupled Integration in Engine Performance Simulations. Int. J. Turbomach. Propuls. Power 2021, 6, 4. https://doi.org/10.3390/ijtpp6010004.

Smith, S. L. (1999). "One-Dimensional Mean Line Code Technique to Calculate Stage-by-Stage Compressor Characteristics. " Master's Thesis, University of Tennessee, 1999.

Cohen H., Rogers G., and Saravanamuttoo H., (1996). Gas Turbine Theory. Longman Group Limited, fourth edition, 1996.

Onder Turan (2009). Compressor Effects on Specific Fuel Consumption of Kerosene-fueled Civil Turbofans. International Journal of Civil Aviation. ISSN 1943-3433 2009, Vol. 1, No. 1: E3 Aircraft Propulsion &Structure Maintenance Department, School of Civil Aviation, Anadolu University, PO Box 26470, Eskisehir, Turkey

APPENDICES

Nomenclature

A blade surface area, m2
Cp specific heat, J/(kg_K)
h total enthalpy,
m inlet mass flow, kg/s
p Pressure, Pa
Q heat energy, J
T Temperature, K
Tc static temperature, K
Tt total (or stagnation) temperature, K
V Velocity, m/s
F = thrust
FAR= fuel air ratio
h = specific enthalpy (kJ/kg)
LHV=lower heating value of fuel (kJ/kgK)
m = mass flow rate of fluid (kg/s)
*m*a = mass flow rate of air at inlet (kg/s)
*m*f = fuel mass flow rate (kg/s)
M = Mach number
p = total pressure (bar)
ps = static pressure (bar)
RpC = compressor pressure ratio (overall)
R = characteristic gas constant
s = specific entropy (kJ/kgK)
SFC= specific fuel consumption (kg/Nh)
T = total temperature (K)
Ts = static temperature (K)
TIT = turbine inlet temperature (K)
W = specific work (kJ/kg)

Greek Symbols

Δp = pressure loss
γ = specific heat ratio
ρ = density
η = efficiency (%)

Suffixes

a = air
amb = ambient
b = burner
g = gas
p = pressure